Macromol. Symp. ***139****, 77–85 (1999)*

Wetting Reversal Transition in Phase-separated Polymer Mixtures

Jan Genzer,*† Jakob Heier and Edward J. Kramer

Materials Department, University of California at Santa Barbara, Santa Barbara,
California, 93106-5050, USA

Abstract: We investigate a wetting reversal transition in thin films of two-phase mixtures of poly(ethylene-propylene) (PEP) and its deuterated analogue (dPEP) on a substrate covered by a self-assembled monolayer (SAM) whose surface energy, γ_{SAM}, is tuned by varying the SAM composition. As γ_{SAM} increases from 21 to 24 mJ/m^2, a transition from a three-layer (air/dPEP/PEP/dPEP/SAM) to a two-layer (air/dPEP/PEP/SAM) structure occurs at increasing T_c - T, where T_c and T are the critical and transition temperatures, respectively. As the system structure changes from three-layer to two-layer, the thicknesses of the dPEP-rich wetting layers at the air/mixture and mixture/SAM interfaces are found to smoothly increase and decrease, respectively, while the thickness of the PEP-rich layer (ca. one half of the total film thickness) does not change. The dependence of the transition temperature on γ_{SAM} is predicted by a simple model using the experimental data on the surface energies of PEP/dPEP and estimates of the interfacial energy between PEP and dPEP.

INTRODUCTION

The behavior of phase-separated polymer blends has been subject of much theoretical and experimental work in the past few years. Upon quenching into the unstable region of the phase diagram, critical mixtures of A and B polymers phase-separate into A-rich and B-rich coexisting phases. In the bulk, the concentration fluctuations that govern the phase separation process are random. As a result, the final morphology consists of interconnected A-rich and B-rich domain structures which coarsen slowly with time (Ref. 1). However, in thin films, the situation changes drastically. The presence of additional interfaces, i.e. the air/mixture and mixture/substrate, causes the directions of the compositional waves in the mixture close to the interfaces to be modified such that the resultant domains are oriented parallel to these interfaces (Refs. 2-6). Hence the phase morphology and its time evolution in thin, phase-separated polymer films are governed by an interplay between phase separation processes and interactions of the A-rich and B-rich polymer phases with the air and with the substrate. While the air surface will always prefer a low surface energy (say, the A-rich phase), the substrate interfacial preference can change from the A-rich phase to the B-rich phase if the

---

[†] Present address: Department of Chemical Engineering, North Carolina State University, Raleigh. North Carolina, 27695-7905, USA.

CCC 1022-1360/99/$ 17.50+.50/0

nature of the substrate surface changes (Refs. 4-6) or, for a constant substrate surface, as the composition of the coexisting phases changes (Ref. 2). Thus if the properties of the substrate surface can be tuned sensitively, it may be possible to observe a transition from an A-rich/B-rich/substrate (two-layer) structure to an A-rich/B-rich/A-rich/substrate (three-layer) structure as the polymer mixture is cooled from the critical temperature. Recently, we experimentally demonstrated that this possibility can be realized using phase-separated mixtures of poly(ethylene-propylene) (PEP) and its deuterated analogue (dPEP) deposited on substrates covered with self-assembled monolayers (SAM) composed of blends of alkanethiols with hydrophobic and hydrophilic end groups (Ref. 7). In this work we present a summary of our recent results and extend our previous investigations to explore the dependence of the thickness of the dPEP-rich wetting layer at the mixture/SAM interface on γ_{SAM} in the vicinity of the three-layer to two-layer transition.

EXPERIMENTAL

Smooth and well characterized substrates are a necessary prerequisite for a precise control of the interactions at the mixture/substrate interface. Such substrates can be fabricated by depositing SAMs of end-functionalized alkanethiols onto gold (Ref. 8). If two thiols having different end groups are coadsorbed onto the Au surface, γ_{SAM} is related to the ratio of the two thiols in the SAM blend. The extent to which the SAM surface energy changes depends on the character of the thiol end groups. When the difference between the polymer/SAM interactions for both phase-separated phases is not substantial, such as in isotopic polymer mixtures, one expects that by varying the surface energy of SAM, one can induce either the A-rich or the B-rich phase to wet the substrate. The substrates for the SAMs were produced by evaporating a layer of Au (ca. 1500 Å thick) onto Si wafers covered with a layer of Cr (ca. 150 Å thick). The latter served as an adhesion promoter for Au. The SAMs were prepared by exposing the Au-covered Si wafers to tetrahydrofuran solutions of $HS(CH_2)_{15}COOH$ / $HS(CH_2)_{17}CH_3$ blends for 24 h at room temperature. After adsorption, the SAMs were washed in tetrahydrofuran and dried with nitrogen. By varying the mole fraction, x, of $HS(CH_2)_{15}COOH$ in the $HS(CH_2)_{17}CH_3$ / $HS(CH_2)_{15}COOH$ blend from 0 to 1, γ_{SAM} increased from ca. 20 to 81 mJ/m^2 (Ref. 7). The values of γ_{SAM} were determined using the geometric mean approximation (GMA) from the measurements of the advancing contact angles, θ, of deionized water and methylene iodide (Ref. 9). The applicability of GMA was checked for by comparing the values of γ_{SAM} with the critical surface energies of SAMs, $\gamma_{SAM,c}$. The latter values were obtained from Zisman plots, which were generated by measuring θ using a series of homologous alkanes (Ref. 7). Our results showed that for $\gamma_{SAM} < 25$ mJ/m^2, the differences between γ_{SAM} and $\gamma_{SAM,c}$ were smaller than 1 mJ/m^2.

The PEP and dPEP polymers were prepared by hydrogenating and deuterating, respectively, anionically polymerized 1,4-polyisoprenes (Ref. 10). The degrees of polymerization of both polymers, N, were ca. 2280, which leads to an upper critical solution temperature, T_c, of ca. 93 °C (Ref. 11). Thin films (ca. 4000 Å thick) of critical dPEP/PEP mixtures (50/50 v/v) were spin-coated from toluene solutions onto glass microscope slides, floated onto a bath of deionized water and picked up with the SAM-covered substrates. The samples were annealed in vacuum at four different temperatures below T_c, namely at 23, 44, 66, and 75 °C, for various times ranging from 4 days (75 °C) to 3 weeks (23 °C). The annealing times were chosen such that the samples reached equilibrium (Ref. 12). After annealing, the samples were quenched by immersion into a bath of liquid nitrogen to preserve the structure. Conventional forward recoil spectrometry (FRES) was then used to measure the volume fraction profiles of dPEP and PEP in the samples (Ref. 13).

RESULTS AND DISCUSSION

Figures 1 and 2 show the volume fraction profiles of dPEP (closed circles) and PEP (open circles) in critical dPEP/PEP mixtures on SAMs made of pure $HS(CH_2)_{17}CH_3$ and pure $HS(CH_2)_{15}COOH$, respectively, annealed at 44 °C for 110 h. The volume fractions of dPEP in the dPEP-rich and the PEP-rich coexisting phases are 0.710 and 0.315, respectively (Ref. 12). Figures 1 and 2 demonstrate that in both samples, a dPEP-rich phase is present at the air/mixture interface, in agreement with previous experiments (Refs. 4,12,14). This behavior is expected because the surface energy of dPEP is lower than that of PEP (Ref. 14). However, depending on the substrate, either a dPEP-rich or a PEP-rich phase is present at the mixture/SAM interface. Namely, for SAMs with $x \leq 0.28$, the mixture/SAM interface is wet by the dPEP-rich phase and for SAMs with $x \geq 0.30$, the mixture/SAM interface is wet by the PEP-rich phase. The transition from the three-layer structure to the two-layer structure thus occurs for SAMs with $0.28 < x < 0.30$ which corresponds to $22.4 < \gamma_{SAM} < 23.5$ mJ/m^2. The crossover from the three-layer to two-layer structure was monitored at three additional annealing temperatures below T_c. The results are presented in the form of the phase diagram of the three-layer to two-layer transitions shown in Fig. 3.

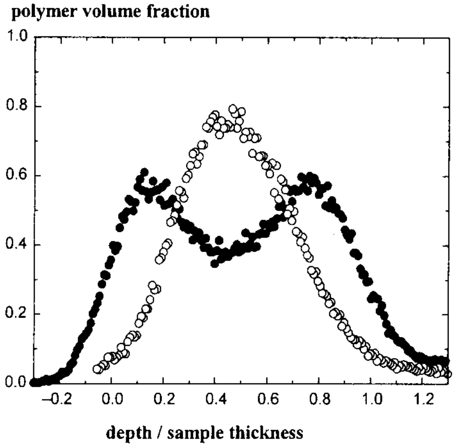

Figure 1 Volume fraction profiles of dPEP (●) and PEP (O) in critical dPEP/PEP mixtures ca. 4000 Å thick at CH_3-terminated SAM annealed at 44 °C for 110 h

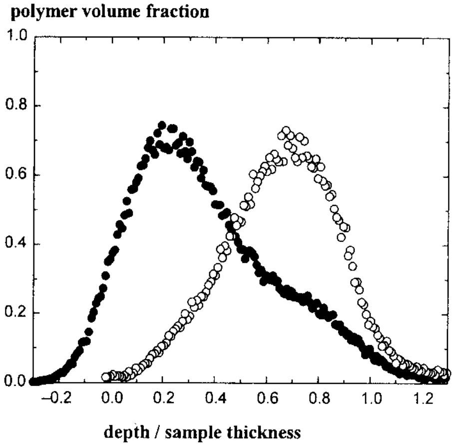

Figure 2 Volume fraction profiles of dPEP (●) and PEP (O) in critical dPEP/PEP mixtures ca. 4000 Å thick at COOH-terminated SAM annealed at 44 °C for 110 h

In Fig. 3, we plot γ_{SAM} as a function of the annealing temperature. The open and solid circles represent the three-layer and two-layer structures, respectively, as determined from the FRES experiments. The solid line is a guide to the eye. The results in Fig. 3 show that with the decreasing quench depth ε ($=1-T/T_c$), the three-layer to two-layer transition takes place at lower values of γ_{SAM}.

Previously we showed that the transition between the three-layer and two-layer structures takes place when

$$\gamma_{SAM/PEP} - \gamma_{SAM/dPEP} = \gamma_{PEP/dPEP} \qquad (1)$$

where $\gamma_{SAM/dPEP}$ and $\gamma_{SAM/PEP}$ are the interfacial energies of the dPEP- and PEP-rich phases and the SAM, respectively, $\gamma_{PEP/dPEP}$ is the interfacial energy between the dPEP- and PEP-rich phases (Ref. 7). We have also demonstrated that γ_{SAM} at which the three-layer to two-layer transition occurs can be estimated from a simple model based on the combination of Young-Dupré and Good-Girifalco equations (Refs. 15,16):

$$\gamma_{SAM} = \{[(\gamma_{PEP} - \gamma_{dPEP}) - (\gamma_{SAM/PEP} - \gamma_{SAM/dPEP})] / [2(\sqrt{\gamma_{PEP}} - \sqrt{\gamma_{dPEP}})]\}^2 \qquad (2)$$

where γ_{PEP} and γ_{dPEP} are the surface energies of the PEP- and dPEP-rich phases. From Eq. (1), $\gamma_{SAM/PEP} - \gamma_{SAM/dPEP}$ can be substituted for by $\gamma_{PEP/dPEP}$ and the latter term evaluated using the expression suggested by Tang and Freed (Ref. 17):

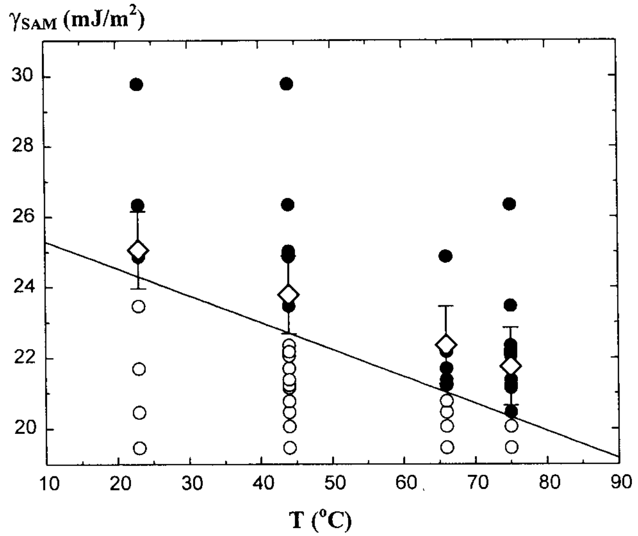

Figure 3 Phase diagram of three-layer to two-layer transitions at the dPEP/PEP mixture/SAM interface for mixtures annealed at four different temperatures below T_c. Also shown are the positions of the three-layer to two-layer transition calculated using the model described in the text and in Ref. 7. (O three-layer structure, ● two-layer structure, ◇ model; the solid line is a guide to the eye)

$$\gamma_{PEP/dPEP} = k_B T a \rho_o (\chi / 6)^{0.5} \left\{ 1 - \frac{1.8}{\chi N} - \frac{0.4}{(\chi N)^2} \right\}^{1.5} \quad (3)$$

In Eq. (3), k_B is the Boltzmann constant, T is absolute temperature, *a* is segment length of the polymers (8 Å), ρ_o is the monomer number density (= 0.0077 Å^{-3}), and χ is the interaction parameter on the coexistence curve between dPEP-rich and PEP-rich phases given by $\chi = 0.16/T - 4.6\text{x}10^{-4}$ (Ref. 12).

The open diamonds in Fig. 3 denote the values of γ_{SAM} calculated using Eqs. (2), (3) and $\gamma_{PEP} - \gamma_{dPEP}$ determined from $\Delta\gamma$, the values of the surface energy difference between PEP and dPEP as a function of the composition of PEP/dPEP mixtures reported by Norton and coworkers (Ref. 14). In the calculations we used $\gamma_{PEP} = 30.6$ mJ/m^2 at 25 °C and $-d\gamma/dT \approx 0.052$ mJ/m^2/K (Ref. 18). The error bars denote the uncertainty in the transition values of γ_{SAM} based on the assumption that the values of γ_{PEP} are known to within ±1 mJ/m^2. The agreement between the measurement and the calculation is excellent, particularly at large ε (low T). At smaller ε, the minor deviations between the measured and calculated γ_{SAM} may be caused by the assumption that $\Delta\gamma$ does not change with temperature. Although the variation of $\Delta\gamma$ with temperature is not expected to be large (Ref. 14), it is evident from Eq. (3) that even a small decrease in $\Delta\gamma$ and thus $\gamma_{PEP} - \gamma_{dPEP}$ with increasing temperature could bring the calculated γ_{SAM} closer to the experimental values.

As previously discussed, at a given ε, the system structure depends on the value of γ_{SAM}. It is of interest to investigate the structural changes as the system moves from the three-layer to two-layer configuration. This can be accomplished by depositing thin films of PEP/dPEP mixtures on SAM substrates whose γ_{SAM}'s span a narrow region around the three-layer to two-layer transition. The SAMs were formed by exposing the Au-covered Si wafers to ethanol solutions of $HS(CH_2)_{11}COOH$ / $HS(CH_2)_{11}CH_3$ blends for 24 h at room temperature. By varying the mole fraction, x, of $HS(CH_2)_{11}COOH$ in the $HS(CH_2)_{11}CH_3$ / $HS(CH_2)_{11}COOH$ blend from 0 to 1, γ_{SAM} increased from ca. 19 to 61 mJ/m^2. Thin films of critical dPEP/PEP mixtures were prepared as previously described. The samples were annealed at 41 °C in vacuum for 7 days and conventional FRES was used to measure the polymer volume fraction profiles. Figure 4 shows the variation of the thickness of the dPEP-rich and PEP-rich wetting layers as evaluated using RUMP (Ref. 19) from the experimental FRES data. From the data in Fig. 3, the three-layer to two-layer transition is expected to occur at γ_{SAM} between 23 and 24 mJ/m^2.

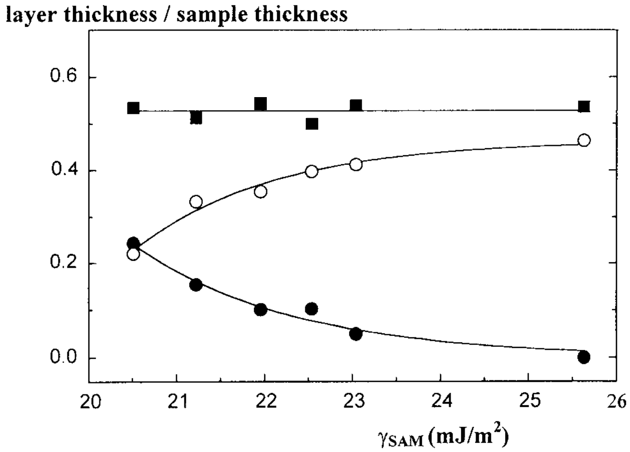

Figure 4 Normalized thickness of the dPEP-rich wetting layers as a function of the surface energy of SAM for samples annealed at 41 °C for 140 h
(● dPEP, mixture/SAM, O dPEP, air/mixture, ■ PEP; the solid lines are guides to the eye)

The results in Fig. 4 show that as γ_{SAM} increases from 20 to 26 mJ/m^2, the thickness of the dPEP-rich layer at the mixture/SAM interface (closed circles) continuously decreases while that of the dPEP-rich layer at the air/mixture (open circles) interface increases. At $\gamma_{SAM} > 23$ mJ/m^2, the system adopts the two-layer structure. Within the resolution of the experiment, the thickness of the PEP-rich wetting layer (closed squares) remains constant over a broad range of γ_{SAM} and is about a half of the total film thickness. This behavior is well understood because the thickness of the PEP-rich layer is fixed by the phase rule. The results shown in Fig. 4 suggest that as γ_{SAM} increases in the vicinity of the three-layer to two-layer transitions, the affinity of dPEP towards the SAM substrate decreases. As γ_{SAM} increases there is a material flow from the mixture/SAM interface across the PEP-rich layer towards the air/mixture interface that builds up the surface dPEP-rich wetting layer.

The main factors that control the thicknesses of the dPEP-rich layers are the strengths of the driving forces governing the segregation of dPEP at the air/mixture and mixture/SAM interfaces. Steiner and Klein recently showed that the growth of wetting layers in thin phase-separated polymer mixtures is driven primarily by long-range surface forces (Ref. 3). The long-range van der Waals energy between two parallel planes is given by $W = -A/(12\pi D^2)$, where A is the Hamaker constant and D is the separation of the planes (Ref. 20). It can be shown (Ref. 21) that within a simple model the thickness of the dPEP-rich layer at the mixture/SAM interface normalized by the total sample thickness, $l_{d,AM}/L$, is given by

$$\frac{l_{d,SAM}}{L} \approx \frac{0.5}{1+\left[\dfrac{\sqrt{\gamma_{PEP}}+\sqrt{\gamma_{dPEP}}}{\sqrt{\gamma_{PEP}}+\sqrt{\gamma_{dPEP}}-2\Phi\sqrt{\gamma_{SAM}}}\right]^{1/3}} \tag{4}$$

where Φ ($\cong 1$) is a Girifalco-Good correction factor accounting for the nature of the intermolecular interactions (Ref. 16). Equation (4) demonstrates that (i) as $\gamma_{SAM} \to 0$, $l_{d,SAM}/L$ approaches 0.25 and (ii) as $\gamma_{SAM} \to \gamma_{dPEP}$, $l_{d,SAM}/L$ decreases to 0. These trends are in accord with the experimental results. At low γ_{SAM} the affinity of dPEP toward the SAM substrate is comparable to that at the air/mixture interface. As a result, the thicknesses of the dPEP-rich wetting layers at both the air/mixture and mixture/SAM interfaces are approximately equal. Upon increasing γ_{SAM}, the system moves closer to the three-layer to two-layer transition and the attraction of dPEP towards the SAM decreases. In this regime, the thickness of the dPEP-rich layer at the mixture/SAM interface decreases and the excess of material is used to build up the dPEP-rich wetting layer at the air/mixture interface.

CONCLUSION

In summary, we have demonstrated that the ultimate phase morphology in thin polymer films can be controlled by suitably adjusting the polymer/substrate interactions and/or the annealing temperature. This control may be exploited in a number of ways. For example, microcontact printing can be used to fabricate a lateral pattern of compositionally different SAMs on the substrate surface. A phase-separated polymer mixture cast on such surfaces may then produce phase structures that are modulated laterally at one temperature but disappear at another one. One could also explore the phase morphologies that will form if the temperature is changed from above the two- to three-layer transition to below it at various stages in the spinodal decomposition process. It seems likely that interesting new morphologies may result.

ACKNOWLEDGMENT

This research was supported by the Division of Materials Research, NSF Polymers Program, under Grant No. NSF-DMR92-23099. The use of the Central Facilities of the Cornell Materials Science Center for the ion beam analysis funded by the NSF-DMR-MRSEC program is acknowledged. We are greatly indebted to Prof. F. S. Bates (University of Minnesota) for supplying PEP and dPEP, Prof. G. M. Whitesides (Harvard University) for donating $HS(CH_2)_{15}COOH$, Dr. J. Srogl (Emory University) for synthesizing $HS(CH_2)_{11}COOH$, and Dr. B. B. Sauer (DuPont) for providing the values of the surface energy of PEP.

REFERENCES

(1) T. Hashimoto, Chap. 6 in *Materials Science and Technology*, Vol. 12, Ed. E. L. Thomas, VCH, Weinheim, 1993, p. 251.

(2) U. Steiner, J. Klein, E. Eiser, A. Budkowski and L. J. Fetters, *Science* **258**, 1126 (1992); U. Steiner, J. Klein and L. J. Fetters, *Phys. Rev. Lett.* **72**, 1498 (1994).

(3) U. Steiner and J. Klein, *Phys. Rev. Lett.* 77, 2526 (1996).

(4) F. Bruder and R. Brenn, *Phys. Rev. Lett.* **69**, 624 (1992).

(5) G. Krausch, C.-A. Dai, E. J. Kramer, J. F. Marko and F. S. Bates, *Macromolecules* **26**, 5566 (1993).

(6) G. Krausch, E. J. Kramer, M. H. Rafailovich and J. Sokolov, *Appl. Phys. Lett.* **64**, 2665 (1994).

(7) J. Genzer and E. J. Kramer, *Phys. Rev. Lett.* **78**, 4946 (1997).

(8) For a recent review of applications of self-assembled monolayers, see D. L. Allara, *Biosens. Bioelectron.* **10**, 771 (1995).

(9) B. B. Sauer and N. V. Dipaolo, *J. Colloid Interface Sci.* **144**, 527 (1991).

(10) A. Zirkel, D. Richter, W. Pyckhout-Hintzen and L. J. Fetters, *Macromolecules* **25**, 954 (1992).

(11) M. D. Gehlsen, J. H. Rosedale, F. S. Bates, G. D. Wignall, L. Hansen and K. Almdal, *Phys. Rev. Lett.* **68**, 2452 (1992).

(12) J. Heier, unpublished results.

(13) For description of conventional FRES, see, e.g.: P. Mills *et al.*, *Appl. Phys. Lett.* **45**, 958 (1984).

(14) L. J. Norton, E. J. Kramer, F. S. Bates, M. D. Gehlsen, R. A. L. Jones, A. Karim, G. P. Felcher and R. Kleb, *Macromolecules* **28**, 8621 (1995).

(15) S. Wu, *Polymer Interface and Adhesion*, Marcel Dekker, New York, 1982.

(16) L. A. Girifalco and R. J. Good, *J. Phys. Chem.* **61**, 904 (1957); *ibid.* **64**, 561 (1960).

(17) H. Tang and K. F. Freed, *J. Chem. Phys.* **94**, 6307 (1991).

(18) B. B. Sauer, to be published.

(19) RUMP is a computer program for simulating the FRES spectra. For details, see L. R. Doolittle, *Nucl. Instrum. Methods Phys. Res., Sect. B* **9**, 344 (1985); *ibid.*, **15**, 227 (1986).

(20) J. Israelachvili, *Intermolecular and Surface Forces*, Academic Press, New York, 1992.

(21) J. Genzer and E. J. Kramer, *Europhys. Lett.* **44**, 180 (1998).